Burgener, L., Hyland, E., Griffith, E., Mitášová, H., Zanno, L.E., and Gates, T.A., 2020, An extreme climate gradient-induced ecological regionalization in the Upper Cretaceous Western Interior Basin of North America: GSA Bulletin, https://doi.org/10.1130/B35904.1.

Supplemental Material

Figure S1. Inverse-distance-weighted (IDW) root mean square error (RMSE) values for different combinations of *n* and *p*, where *n* is the number of neighboring temperature values included in the weighted average estimate, and *p* is the weight or power parameter applied to each neighbor. The combination of *n* and *p* that resulted in the lowest RMSE were chosen for the final IDW calculations reported in this study. Note that a jitter factor was applied to the x-axis values of data to improve readability.

Figure S2. Latitudinal MAT transects and associated uncertainties from the Monte Carlo simulations, for the Campanian (A), early Maastrichtian (B), and late Maastrichtian (C) analysis windows. The solid lines show the mean MAT values for the western edge (red), center (blue), and eastern edge (green) of the study areas. The shaded regions show the maximum and minimum range of the 1000 unique interpolated temperature maps.

Figure S3. Raw fossil pollen (A, B, C) and leaf (D, E, F) bar charts showing differences in north/south ecoregion abundances.

Figure S4. Spatial patterns in fossil pollen (A-C) and leaf (D-F) ecoregion abundances. Abundance categories I, II, III, and IV indicate the mean, minimum, and minimum interpolated abundances for each ecoregion type.

DETAILED METHODS AND MATERIALS

1. Temperature estimate uncertainties

The uncertainties associated with each individual MAT estimate were combined into a total MAT uncertainty using a root sum of squares method:

$$u_c(T) = \sqrt{\Sigma_i (u(T_i))^2} \quad (1)$$

where $u_c(T)$ is the combined standard uncertainty, and $u(T_i))^2$ is the uncertainty associated with the individual MAT estimate T_i.

2. Raw versus adjusted temperature estimates

Three analysis windows were chosen with the goal of minimizing the amount of time averaging imposed on our interpolations, while still retaining sufficient (at least 10) unique sample localities for the spatial interpolation calculations (Table S1). Because two of these analysis windows (Campanian and late Maastrichtian) still covered more than 2 million years, we used the global Cretaceous temperature curves of Friedrich et al. (2012) and O'Brien et al. (2017) to adjust our temperature data to account for secular changes to global MAT. The mean difference between the interpolations using the raw temperature data versus the adjusted temperature data is –1 °C (–1.5 to –0.4 °C) for the Campanian analysis window, –0.1 °C (–0.67–0.56 °C) for the early Maastrichtian analysis window, and –0.76 °C (–1.5 to –0.4) for the late Maastrichtian analysis window. Because the difference between the raw and adjusted temperatures are small and within the range of uncertainty, we report only the raw temperature interpolations in this study.

3. Spatial interpolation methods

Spatially interpolated maps of MAT were created for each analysis window using the inverse distance weighted (IDW) method (Shepard, 1968) as implemented in the custom MATLAB function gIDW (Langella, 2020) which estimates a value (e.g., MAT) for an unsampled location based on the weighted average of surrounding, sampled points using the following equation:

$$T_j = \frac{\Sigma_i^n \frac{T_i}{d_{ij}^p}}{\Sigma_i^n \left(\frac{1}{d_{ij}^p}\right)} \quad (2)$$

where T_j is the estimated MAT at unsampled location j, T_i is a known MAT at sampled location i, d_{ij} is the distance between locations j and i, n is the number of sampled locations or neighbors included in the weighted average, and p is the weight or power parameter applied to d_{ij} as an exponent such that as d_{ij} increases in magnitude, the effect of T_i on T_j decreases. Using this equation, the final estimated value of T_j can be adjusted by changing p and n.

Root mean square errors (RMSE) were calculated for the interpolations by using a jackknife resampling approach. This involved removing one sample from our paleotemperature data set, performing the IDW interpolation with the remaining samples, and then comparing the estimated temperature at the location of the removed sample to the actual reconstructed value. This process was then repeated for each sample in the paleotemperature data set. Final p and n values were then chosen to minimize RMSE for each analysis window (Fig. S1).

We chose to use the relatively simple IDW method rather than a more complex statistical interpolation method such as Kriging for two reasons. First, the structural analysis of our temperature data sets did not produce semivariogram results that fit well with any commonly used semivariogram models (e.g., circular, spherical, exponential, linear, etc.). Second, the Kriging results were consistent with the IDW results, and did not provide any additional information.

4. Identifying MAT transition zones

For the purposes of this study, we define a transition zone as a contiguous latitudinal zone with a mean slope that is significantly more negative than the mean Late Cretaceous latitudinal temperature gradient (–0.3 to –0.4 °C °lat^{-1}, 4). For each of the 1000 Monte Carlo IDW iterations calculated for the three MAT data sets, latitudinal MAT transects were analyzed at 1° longitude intervals. The script identifies contiguous areas of negative MAT slopes along each transect where at least one cell has a slope more negative than some threshold temperature slope (see below). Cells within the identified latitudinal zone were then assigned a value of 1, while cells outside the zone were assigned a value of 0. By summing the results of this analysis for the 1000 Monte Carlo iterations, we were able to identify how often a given cell was identified as being inside the steep latitudinal gradient zone (e.g., Fig. S3). Cells that were flagged as being within the steep latitudinal gradient zone in at least 70% of the Monte Carlo iterations were than considered to be within the transition zone. These calculations were performed using three different slope threshold values: –0.3 °C °lat^{-1} (minimum estimated Late Cretaceous temperature gradient), –0.4 °C °lat^{-1} (maximum estimated Late Cretaceous temperature gradient), and –0.5 °C °lat^{-1} (conservative temperature gradient estimate).

Latitudinal temperature gradients were calculated for each longitudinal transect in the 1000 iterations of the Campanian, early Maastrichtian, and late Maastrichtian spatial interpolations using the following multivariate linear regression model:

$$MAT = b_0 + (b_1 \times L) + (b_2 \times TZ) + (b_3 \times L{:}TZ) + \varepsilon \quad (3)$$

where L is the paleolatitude, TZ is an identifier variable that indicates whether a given cell is inside or outside the previously described temperature transition zone, $L{:}TZ$ is an interaction variable between L and TZ, and ε is the error term associated with the linear regressions. The regression coefficients b_0, b_1, b_2, and b_3 are associated with L, TZ, and L:TZ, respectively. The interaction effect allows for two separate lines to be fit to the data, depending on whether a given cell is inside or outside the transition zone. For cells outside the transition zone, b_0 is the y-intercept value and b_1 is the change in MAT for a one unit increase in paleolatitude. For cells inside the transition zone, $b_0 + b_2$ is the y-intercept value and $b_1 + b_3$ is the change in MAT for a one unit increase in paleolatitude.

5. Fossil pollen and leaf ecoregion assignment

Ecoregions simplified for paleo-applications were defined based on available information for sample localities (c.f., USDA Levels I and II). For sites where authors provided a detailed environment and/or ecosystem description, this was conserved in our analysis. For sites where no such description was provided, both depositional environment (either from the original study, or compiled from the Paleobiology Database; PBDB data downloaded from the Paleobiology Database on April 9, 2020) and floral assemblage (from the original study) were used to define

an ecoregion. For floral assemblages (both pollen and leaf), an ecoregion was identified by attributing fossil taxa to a modern nearest living relative (unattributed or disputed groups assigned conservatively at higher taxonomic levels), and then linking modern distributions (Omernik and Griffith, 2014) to existing low-resolution ecoregion maps. For consistency, this method was verified against ecoregion designations for which authors provided an original description, and any discrepancies or unattributable groups are noted in Data sets S3 and S4.

6. Fossil pollen and leaf Dice Similarity analysis

Pairwise comparisons of biodiversity using the Dice Similarity Index were performed in the R package *fossil* version 0.4.0 (Vavrek and Larsson, 2010). The resulting data set contained the similarity value between each formation for which pollen and leaf data was known (each data set analyzed separately), as well as the geodesic line distance between them (also from the R package *fossil* version 0.4.0), mean age of the formation, and the time gap between each pair of formations.

7. Floral climatic boundary test

Using the shift in temperature transition zones as a guide, we tested each integer of latitude from 40 to 60 degrees as being a potential boundary zone within a two-zone biogeographical distribution of plants during the latest Cretaceous of North America. If after assessing results from each of these latitudes it is found that the pattern expected of a bizonal or transitional biotic zonation is not present, then this would be evidence that the climatic boundary observed from climate proxies did not affect the distribution of plant species.

In order to test the hypothesis that a climatic barrier caused two distinct biomes of vegetation, we filtered the similarity results data set into three subsets, 72 – 80 Ma, 69 – 78 Ma, and 66 – 75 Ma. The broad time bins for this analysis were required in order to achieve an adequate sample size for calculations, although we did limit the inclusion of pairwise similarity results to those formations that are separated by three million years or less. An advantage to using broad time bins is that results will be homogenized over a larger amount of time data, meaning that any data excursions within smaller time frames will be suppressed by data from other time frames, thereby producing smoother, more conserved, variation within the pairwise similarity indices. For each of the 20 test latitudes we categorized formations whose paleolatitude fell north or south of the hypothesized boundary into respective North or South bins. Each pairwise similarity calculation was, therefore, labeled as a North-North, North-South, or South-South comparison.

This test was designed to determine the amount of statistical variation of pairwise similarity within and between hypothesized biomes. Consider a geographic area that is divided into two latitudinally-arrayed biogeographical biomes with a small zone of transition between the biomes. Additionally, within each biome there are several localities that preserve a particular set of organisms on which similarity calculations are to be made. If one were to choose a latitude and then calculate pairwise similarity between each of the localities within the northern and southern biomes, a certain amount of statistical variation would exist among the similarity values that is contingent upon the amount of mixing occurring within the true northern and southern biomes that are incorrectly lumped together within the hypothetical northern or hypothetical southern zones currently being tested. In other words, the greater the amount of inappropriately

categorized fauna/flora within a single hypothetical biome, the larger the statistical variance present within the similarity values of a particular zone. Likewise, for those pairwise comparisons that cross a biome boundary, we would expect to see greater variance in the distribution of similarity values closer to the biome boundary, because localities that are in actuality closely related but incorrectly classified in the opposite biome, will be more similar to one another and therefore decrease the overall statistical variance. In short, we ran consecutive tests of within- and between-biome variance, suggesting that the true biotic boundary—if present—would be found at the position that maximizes the difference between in-group variance (i.e., the absolute value of the difference between the northern and southern similarity variance) and between-group variance. Additionally, we posit that the boundaries of a transitional zone can be estimated by finding the latitudes where the solution to the equation (between-group variance – in-group variance) is minimized (note that this is not the same as the absolute value of the difference).

One problem with this sliding window approach is that near the extremes of the test windows we will have far more formations present in one biome versus another when calculating variance. To accommodate this inequity, we randomly sampled 100 populations from the larger of the two biomes that were equal in size to the population in the smaller biome. All values from the subsampling and the raw cross-boundary variances were estimated and plotted with LOESS. These values were then standardized to 1 for plotting.

SUPPLEMENTARY INFORMATION REFERENCES CITED

Friedrich, O., Norris, R.D., and Erbacher, J., 2012, Evolution of middle to Late Cretaceous oceans—A 55 m.y. record of Earth's temperature and carbon cycle: Geology, v. 40, no. 2, p. 107–110, https://doi.org/10.1130/G32701.1.

O'Brien, C.L., Robinson, S.A., Pancost, R.D., Sinninghe Damste, J.S., Schouten, S., Lunt, D.J., Alsenz, H., Bornemann, A., Bottini, C., Brassell, S.C., Farnsworth, A., Forster, A., Huber, B.T., Inglis, G.N., Jenkyns, H.C., Linnert, C., Littler, K., Markwick, P., Mcanena, A., Mutterlose, J., Naafs, B.D.A., Püttmann, W., Sluijs, A., Van Helmond, N.A.G.M., Vellekoop, J., Wagner, T., and Wrobel, N.E., 2017, Cretaceous sea-surface temperature evolution: Constraints from TEX 86 and planktonic foraminiferal oxygen isotopes: Earth-Science Reviews, v. 172, no. July, p. 224–247, https://doi.org/10.1016/j.earscirev.2017.07.012.

Langella, G., 2020, Inverse Distance Weighted (IDW) or Simple Moving Average (SMA) Interpolation: MATLAB Central File Exchange. https://www.mathworks.com/matlabcentral/fileexchange/27562-inverse-distance-weighted-idw-or-simple-moving-average-sma-interpolation?focused=5152732&tab=function

Omernik, J.M., and Griffith, G.E., 2014, Ecoregions of the Conterminous United States: Evolution of a hierarchical spatial framework: Environmental Management, v. 54, p. 1249–1266, https://doi.org/10.1007/s00267-014-0364-1.

Shepard, D., 1968, A two-dimensional interpolation function for irregularly-spaced data: Proceedings-1968 ACM National Conference, p. 517–524.

Vavrek, M.J., and Larsson, H.C.E., 2010, Low beta diversity of Maastrichtian dinosaurs of North America: Proceedings of the National Academy of Sciences of the United States of America, v. 107, no. 18, p. 8265–8268, https://doi.org/10.1073/pnas.0913645107.

Temperature data files references

Amiot, R., Lécuyer, C., Buffetaut, E., Fluteau, F., Legendre, S., and Martineau, F., 2004, Latitudinal temperature gradient during the Cretaceous Upper Campanian-Middle Maastrichtian: δ18O record of continental vertebrates: Earth and Planetary Science Letters, v. 226, no. 1–2, p. 255–272, https://doi.org/10.1016/j.epsl.2004.07.015.

Barrick, R.E., Fischer, A.G., and Showers, W.J., 1999, Oxygen Isotopes from Turtle Bone: Applications for Terrestrial Paleoclimates?: Palaios, v. 14, no. 2, p. 186–191, https://doi.org/10.2307/3515374.

Burgener, L.K., Hyland, E.G., Huntington, K.W., Kelson, J.R., and Sewall, J.O., 2019, Revisiting the Equable Climate Problem During the Late Cretaceous Greenhouse Using Paleosol Carbonate Clumped Isotope Temperatures from the Campanian Western Interior Basin: Palaeogeography, Palaeoclimatology, Palaeoecology, v. 516, p. 244–267, https://doi.org/10.1016/j.palaeo.2018.12.004.

Carpenter, S.J., Erickson, J.M., and Holland, F.D.J., 2003, Migration of a Late Cretaceous fish: Nature, v. 423, no. 70–74.

Dworkin, S.I., Nordt, L., and Atchley, S., 2005, Determining terrestrial paleotemperatures using the oxygen isotopic composition of pedogenic carbonate: Earth and Planetary Science Letters, v. 237, p. 56–68, https://doi.org/10.1016/j.epsl.2005.06.054.

Estrada-ruiz, E., and Upchurch, G., 2008, Flora and climate of the Olmos Formation (Upper Campanian-Lower Maastrichtian), Coahuila, Mexico: a preliminary report: Gulf Coast Association of Geological Societies Transactions, v. 58, p. 273–283.

Golovneva, L.B., 2000, The Maastrichtian (Late Cretaceous) climate in the Northern Hemisphere, *in* Hart, M., eds., Climates: Past and Present: London, Geological Society, Special Publications, p. 43–54, https://doi.org/10.1144/GSL.SP.2000.181.01.05.

Johnson, K.R., Reynolds, M.L., Werth, K.W., and Thomasson, J.R., 2003, Overview of the Late Cretaceous, early Paleocene, and early Eocene megafloras of the Denver Basin, Colorado: Rocky Mountain Geology, v. 38, no. 1, p. 101–120, https://doi.org/10.2113/gsrocky.38.1.101.

Miller, I.M., Johnson, K.R., Kline, D.E., Nichols, D.J., and Barclay, R.S., 2013, A Late Campanian flora from the Kaiparowits Formation, southern Utah, and a brief overview of the widely sampled but little-known Campanian vegetation of the Western Interior of North America, *in* Titus, A.L., and Loewen, M.A., eds., At the Top of the Grand Staircase: Bloomington, Indiana: Indiana University Press.

Oliver, S., 2010, Digital leaf physiognomy: correlating leaf size and shape to climate in the Fox Hills, Fort Union, and Hanna Basin Formations: Wesleyan University.

Peppe, D.J., Royer, D.L., Cariglino, B., Oliver, S.Y., Newman, S., Leight, E., Enikolopov, G., Fernandez-Burgos, M., Herrera, F., Adams, J.M., Correa, E., Currano, E.D., Erickson, J.M., Hinojosa, L.F., Hoganson, J.W., Iglesias, A., Jaramillo, C.A., Johnson, K.R., Jordan, G.J., Kraft, N.J.B., Lovelock, E.C., Lusk, C.H., Niinemets, U., Penuelas, J., Rapson, G., Wing, S.L., and Wright, I.J., 2011, Sensitivity of leaf size and shape to climate: global patterns and paleoclimatic applications: The New Phytologist, v. 190, no. 3, p. 724–739, https://doi.org/10.1111/j.1469-8137.2010.03615.x.

Petersen, S.V., Tabor, C.R., Lohmann, K.C., Poulsen, C.J., Meyer, K.W., Carpenter, S.J., Erickson, J.M., Matsunaga, K.K.S., Smith, S.Y., and Sheldon, N.D., 2016, Temperature and salinity of the Late Cretaceous Western Interior Seaway Estimates of WIS Temperature: Geology, v. 44, no. 11, p. 903–906, https://doi.org/10.1130/G38311.1.

Prue, A.M.A., 2018, Paleoclimate of the Two Medicine Formation based on leaf physiognomy: Texas State University.

Quinney, A., Therrien, F., Zelenitsky, D.K., and Eberth, D.A., 2013, Palaeoenvironmental and palaeoclimatic reconstruction of the Upper Cretaceous (late Campanian – early Maastrichtian) Horseshoe Canyon Formation, Alberta, Canada: Palaeogeography, Palaeoclimatology, Palaeoecology, v. 371, p. 26–44, https://doi.org/10.1016/j.palaeo.2012.12.009.

Snell, K.E., Koch, P.L., Druschke, P., Foreman, B.Z., and Eiler, J.M., 2014, High elevation of the "Nevadaplano" during the Late Cretaceous: Earth and Planetary Science Letters, v. 386, p. 52–63, https://doi.org/10.1016/j.epsl.2013.10.046.

Spicer, R.A., and Herman, A.B., 2010, The Late Cretaceous environment of the Arctic: A quantitative reassessment based on plant fossils: Palaeogeography, Palaeoclimatology, Palaeoecology, v. 295, no. 3–4, p. 423–442, https://doi.org/10.1016/j.palaeo.2010.02.025.

Tobin, T.S., Wilson, G.P., Eiler, J.M., and Hartman, J.H., 2014, Environmental change across a terrestrial Cretaceous-Paleogene boundary section in eastern Montana, USA, constrained by carbonate clumped isotope paleothermometry: Geology, v. 42, no. 4, p. 351–354, https://doi.org/10.1130/G35262.1.

Upchurch, G.R., Kiehl, J., Shields, C., Scherer, J., and Scotese, C., 2015, Latitudinal temperature gradients and high-latitude temperatures during the latest Cretaceous: Congruence of geologic data and climate models: Geology, v. 43, no. 8, p. 683–686, https://doi.org/10.1130/G36802.1.

Van Boskirk, M.C., 1998, The flora of the Eagle Formation and its significance for Late Cretaceous floristic evolution: Yale University.

Wilf, P., Johnson, K.R., and Huber, B.T., 2003, Correlated terrestrial and marine evidence for global climate changes before mass extinction at the Cretaceous – Paleogene boundary: Proceedings of the National Academy of Sciences of the United States of America, v. 100, no. 2, p. 599–604, https://doi.org/10.1073/pnas.0234701100.

[[CrossRef reports the first author should be "Wolf", not "Wolfe"]]Wolfe, J.A., 1990, Palaeobotanical evidence for a marked temperature increase following the Cretaceous/Tertiary boundary: Nature, v. 343, p. 153–156, https://doi.org/10.1038/343153a0.

Wolfe, J.A., Upchurch, G.R., Survey, U.S.G., and Co, U.S.A., 1987, North American nonmarine climates and vegetation during the Late Cretaceous: Palaeogeography, Palaeoclimatology, Palaeoecology, v. 61, p. 33–77, https://doi.org/10.1016/0031-0182(87)90040-X.

Zakharov, Y.D., Popov, A.M., Shigeta, Y., Smyshlyaeva, O.P., Sokolova, E.A., Nagendra, R., et al., 2006, New Maastrichtian oxygen and carbon isotope record: Additional evidence for warm low latitudes: Geosciences Journal, v. 10, no. 3, p. 347–367, https://doi.org/10.1007/BF02910375.

Fossil Pollen data files references

Anderson, R.Y., 1960, Cretaceous-Tertiary Palynology, Eastern Side of the San Juan Basin, New Mexico, *in* Memoir 6: Socorro, New Mexico Bureau of Mines & Mineral Resources.

Arens, N.C., Thompson, A., and Jahren, A.H., 2014, A preliminary test of the press-pulse extinction hypothesis: Palynological indicators of vegetation change preceding the Cretaceous-Paleogene boundary, McCone County, Montana, USA: The Geological Society of America Special Paper 503, p. 209–227, https://doi.org/10.1130/2014.2503(07).

Bercovici, A., Pearson, D., Nichols, D., and Wood, J., 2009, Biostratigraphy of selected K/T boundary sections in southwestern North Dakota, USA: toward a refinement of palynological identification criteria: Cretaceous Research, v. 30, no. 3, p. 632–658, https://doi.org/10.1016/j.cretres.2008.12.007.

Bihl, G., 1973, Palynostratigraphic investigation of Upper Maastrichtian and Paleocene strata near Tate Lake, N.W.T.: The University of British Columbia.

Braman, D.R., and Koppelhus, E.B., 2005, Campanian Palynomorphs. In Dinosaur Provincial Park: A Spectacular Ancient Ecosystem Revealed: Bloomington, Indiana, p. 101–130.

Clarke, R.T., 1963, Palynology of Vermejo Formation Coals (Upper Cretaceous) in the Canon City Coal Field, Fremont County: Colorado, The University of Oklahoma.

Farabee, M.J., and Canright, J.E., 1986, Stratigraphic palynology of the lower part of the Lance Formation (Maestrichtian) of Wyoming: Palaeontographica. Abteilung B, Paläophytologie, v. 199, no. 1–3, p. 1–89.

Fouch, T., 1983, Patterns and timing of synorogenic sedimentation in Upper Cretaceous rocks of central and Northeast Utah: Rocky Mountain Paleogeography Symposium, 2, p. 305–338.

Franczyk, K.J., Pitman, J.K., and Nichols, D.J., 1990, Sedimentology, mineralogy, palynology, and depositional history of some Uppermost Cretaceous and Lowermost Tertiary rocks along the Utah Book and Roan Cliffs east of the Green River. In U.S. Geological Survey Bulletin 1787: Denver, Evolution of Sedimentary Basins-Uinta and Piceance Basins, p. 1–36.

Frederiksen, N.O., Ager, T.A., and Edwards, L.E., 1988, Palynology of Maastrichtian and Paleocene rocks, lower Colville River region, North Slope of Alaska: Canadian Journal of Earth Sciences, v. 25, no. 4, p. 512–527, https://doi.org/10.1139/e88-051.

Gallucci, R.N., 1986, Palynology and Biostratigraphy of the Upper Cretaceous Adaville Formation (southwestern Wyoming) and Biostratigraphic Comparison to the Niobrara Formation: Ridgway, Colorado, Idaho State University.

Jarzen, D., 1982, Palynology of Dinosaur Provincial Park (Campanian), Alberta: Syllogeus, v. 38, p. 1–69, 10.1017/CBO9781107415324.004.

Kroeger, T.J., 2002, Palynology of the Hell Creek Formation (Upper Cretaceous, Maastrichtian) in northwestern South Dakota: Effects of paleoenvironment on the composition of palynomorph assemblages: In Geological Society of America Special Paper 361, p. 457–472.

Leffingwell, H.A., 1970, Palynology of the Lance (Late Cretaceous) and Fort Union (Paleocene) formations of the type Lance area, Wyoming: Geological Society of America. Special Paper, v. 127, p. 1–64, https://doi.org/10.1130/SPE127-p1.

Lerbekmo, J.F., Sweet, A.R., and St. Louis, R.M., 1987, The relationship between the iridium anomaly and palynological floral events at three Cretaceous-Tertiary boundary localities in western Canada: Geological Society of America Bulletin, v. 99, no. 3, p. 325–330, https://doi.org/10.1130/0016-7606(1987)99<325:TRBTIA>2.0.CO;2.

Lohrengel, C.F., 1969, Palynology of the Kaiparowits Formation, Garfield County, Utah: Geology Studies, v. 16, no. 3.

May, F.E., 1972, A survey of palynomorphs from several coal-bearing horizons of Utah, *in* Doelling, H.H., ed., Central Utah coal fields: Sevier-Sanpete, Wasatch Plateau, Book Cliffs and Emery: Salt Lake City, Utah, p. 497–542.

Miller, I.M., Johnson, K.R., Kline, D.E., Nichols, D.J., and Barclay, R.S., 2013, A Late Campanian flora from the Kaiparowits Formation, southern Utah, and a brief overview of

the widely sampled but little-known Campanian vegetation of the Western Interior of North America, *in* Titus, A.L., and Loewen, M.A., eds., At the Top of the Grand Staircase. Bloomington, Indiana: Indiana University Press.

Nichols, D.J., and Bryant, B., 1986, Palynology of the Currant Creek and Mesaverde Formations in the Currant Creek-Duchesne River area, Duchesne and Wasatch counties, Utah; Open-file report 86–160.

Nichols, D.J., and Bryant, B., 1986, Palynologic data from Cretaceous and early Tertiary rocks in the Salt Lake 30' × 60' quadrangle: Open-file report 86–116.

Payenberg, T.H.D., Braman, D.R., David, D.W., and Miall, A.D., 2002, Litho- and chronostratigraphic relationships of the Santonian-Campanian Milk: Canadian Journal of Earth Sciences, v. 39, no. 10, p. 1553–1577, https://doi.org/10.1139/e02-050.

Peppe, D., 2003, Fox Hills I, a new Upper Maastrichtian megafloral zone within the Williston Basin of North Dakota. St. Lawrence University.

Radforth, N.W., and Rouse, G.E., 1953, The classification of recently discovered Cretaceous plant microfossils of potential importance to the stratigraphy of Western Canadian coals: Canadian Journal of Botany, v. 32, p. 187–201, https://doi.org/10.1139/b54-017.

Roberts, A.E., 1972, Cretaceous and Early Tertiary depositional and tectonic history of the Livingston area, Southwestern Montana: Geological Survey Professional Paper 526-C.

Skipp, B., and McGrew, L.W., 1977, The Maudlow and Sedan Formations of the Upper Cretaceous Livingston Group on the west edge of the Crazy Mountains Basin, Montana: U.S. Geological Survey Bulletin 1422-B, 76.

Snead, R.G., 2006, Microfloral diagnosis of the Cretaceous-Tertiary boundary, central Alberta: Research Council of Alberta, p. 0–25.

Srivastava, S., 1966, Upper Cretaceous microflora (Maestrichtian) from Scollard, Alberta, Canada: Pollen et Spores, v. 8, no. 3, p. 497–552.

Srivastava, S.K., 1967, Palynology of Late Cretaceous Mammal Beds, Scollard, Alberta (Canada): Palaeogeography, Palaeoclimatology, Palaeoecology, v. 3, p. 133–150, https://doi.org/10.1016/0031-0182(67)90010-7.

Srivastava, S.K., and Braman, D.R., 2013, The palynostratigraphy of the Edmonton Group (Upper Cretaceous) of Alberta, Canada: Palynology, v. 37, no. 1, p. 1–27, https://doi.org/10.1080/01916122.2012.673288.

Stanley, E.A., 1965, Upper Cretaceous and Paleocene plant microfossils and Paleocene dinoflagellates and hystrichosphaerids from northwestern South Dakota: Bulletins of American Paleontology, v. 49, no. 222, p. 179–379.

Stone, J.F., 1971, Palynology of the Almond Formation (Upper Cretaceous), Rock Springs Uplift, Wyoming: Michigan State University.

Tschudy, B.D., 1973, Palynology of the Upper Campanian (Cretaceous) Judith River Formation, North-Central Montana: Geological Survey Professional Paper, v. 770, p. 1–72, https://doi.org/10.3133/pp770.

Tschudy, R.H., 1973, The Gasbuggy Core- A Palynological Appraisal. In Cretaceous and Tertiary Rocks of the Southern Colorado Plateau, Four Corners Geological Society Memoir Book: American Association of Petroleum Geologists, p. 131–143.

Wolberg, D.L., 1980, Data base and review of paleofaunas and floras of the Fruitland Formation, Late Cretaceous, San Juan Basin, New Mexico, with interpretive observations and age relationships: Socorro, Open File Report 117.

Fossil leaf data file references

Arens, N.C., and Allen, S.E., 2014, A florule from the base of the Hell Creek Formation in the type area of eastern Montana: implications for vegetation and climate, *in* Through the End of the Cretaceous in the Type Locality of the Hell Creek Formation in Montana and Adjacent Areas: Geological Society of America Special Paper 503, p. 173–207.

Crabtree, D.R., 1987, The early Campanian flora of the Two Medicine Formation, northcentral Montana: University of Montana.

Dawson, J.W., 1886, On the fossil plants of the Laramie Formation of Canada. In Royal Society of Canada Transactions, Section IV: Geological and Biological Sciences.

Dorf, E., 1955, Paleobotanical correlations of Late Cretaceous deposits in southwestern Wyoming, Tenth Annual Field Conference-1955: Wyoming Geological Association Guidebook.

Hunt, A.P., and Lucas, S.G., 1992, Stratigraphy, paleontology and age of the Fruitland and Kirtland Formations (Upper Cretaceous), San Juan Basin, New Mexico, *in* Lucas, S.G., Kues, B.S., Williamson, T.E., and Hunt, A.P., eds., San Juan Basin IV: New Mexico Geological Society 43rd Annual Fall Field Conference Guidebook, p. 217–239.

Johnson, K.R., 2002, Megaflora of the Hell Creek and lower Fort Union Formations in the western Dakotas: vegetational response to climate change, the Cretaceous-Tertiary boundary event, and rapid marine transgression: Geological Society of America. Special Paper, v. 361, p. 329–391, https://doi.org/10.1130/0-8137-2361-2.329.

Johnson, K.R., 1992, Leaf-fossil evidence for extensive floral extinction at the Cretaceous-Tertiary boundary, North Dakota, USA: Cretaceous Research, v. 13, no. 1, p. 91–117, https://doi.org/10.1016/0195-6671(92)90029-P.

Johnson, K.R., 1989, A high-resolution megafloral biostratigraphy spanning the Cretaceous-Tertiary boundary in the northern Great Plains: Yale University.

Knowlton, F.H., 1916, Flora of the Fruitland and Kirtland Formations, *in* Shorter Contributions to General Geology: U.S. Geological Survey, p. 241–258.

Knowlton, F.H. 1916, The flora of the Fox Hills Sandstone: Shorter Contributions to General Geology.

Knowlton, F.H., 1900, Flora of the Montana Formation: Bulletin of the United States Geological Survey, no. 163, 10.1021/i500006a614.

Knowlton, F.H., 1905, Fossil Plants: U.S. Geological Survey Bulletin No. 257: Geology and Paleontology of the Judith River Beds, https://doi.org/10.5479/si.00810266.90.1

McIver, E.E., 1999, Paleobotanical evidence for ecosystem disruption at the Cretaceous-Tertiary boundary from Wood Mountain, Saskatchewan, Canada: Canadian Journal of Earth Sciences, v. 36, no. 5, p. 775–789, https://doi.org/10.1139/e97-112.

Parker, L.R., 1976, The paleoecology of the fluvial coal-forming swamps and associated floodplain environments in the Blackhawk Formation (Upper Cretaceous) of Central Utah: Geology Studies, v. 22, no. 3, p. 99–116.

Peppe, D.J., Erickson, J.M., and Hickey, L.J., 2007, Paleontological Society Fossil Leaf Species from the Fox Hills Formation (Upper Cretaceous: North Dakota, USA) and Their Paleogeographic Significance: Journal of Paleontology, v. 81, no. 3, p. 550–567.

Richardson, G.B., 1909, Reconnaissance of the Book Cliffs Coal Field between Grand River, Colorado and Sunnyside, Utah: U.S. Geological Survey Bulletin, 371 p.

Robison, C., Hunt, A., and Woldberg, D., 1982, New Late Cretaceous leaf locality from lower Kirtland Shale member, Bisti area, San Juan Basin, New Mexico: New Mexico Geology, v. 4, no. 3, p. 42–46.

Rouse, G.E., 1967, Late Cretaceous Plant Assemblage From East-Central British Columbia: I, Fossil Leaves: Canadian Journal of Earth Sciences, v. 4, no. 6, p. 1185–1197, https://doi.org/10.1139/e67-080.

Skipp, B., and McGrew, L.W., 1977, The Maudlow and Sedan Formations of the Upper Cretaceous Livingston Group on the west edge of the Crazy Mountains Basin, Montana: U.S. Geological Survey Bulletin 1422-B, 76 p.

Tidwell, W.D., Ash, S.R., and Parker, L.R., 1981, Cretaceous and Tertiary floras of the San Juan Basin: Advances in San Juan Basin Paleontology: Albuquerque, University of New Mexico Press, p. 307–332.

Van Boskirk, M.C., 1998, The flora of the Eagle Formation and its significance for Late Cretaceous floristic evolution: Yale University.

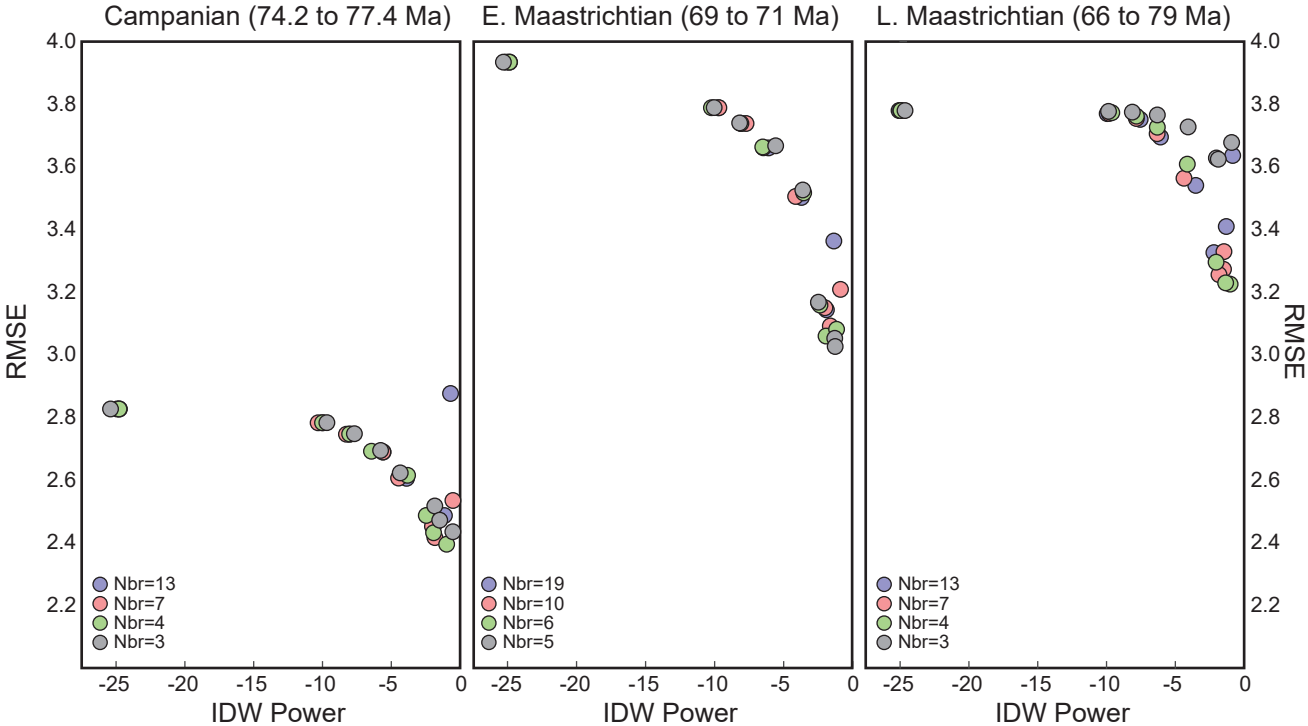
Campanian (74.2 to 77.4 Ma)
E. Maastrichtian (69 to 71 Ma)
L. Maastrichtian (66 to 79 Ma)
RMSE
IDW Power
4.0
3.8
3.6
3.4
3.2
3.0
2.8
2.6
2.4
2.2
-25
-20
-15
-10
-5
0
Nbr=13
Nbr=7
Nbr=4
Nbr=3
Nbr=19
Nbr=10
Nbr=6
Nbr=5

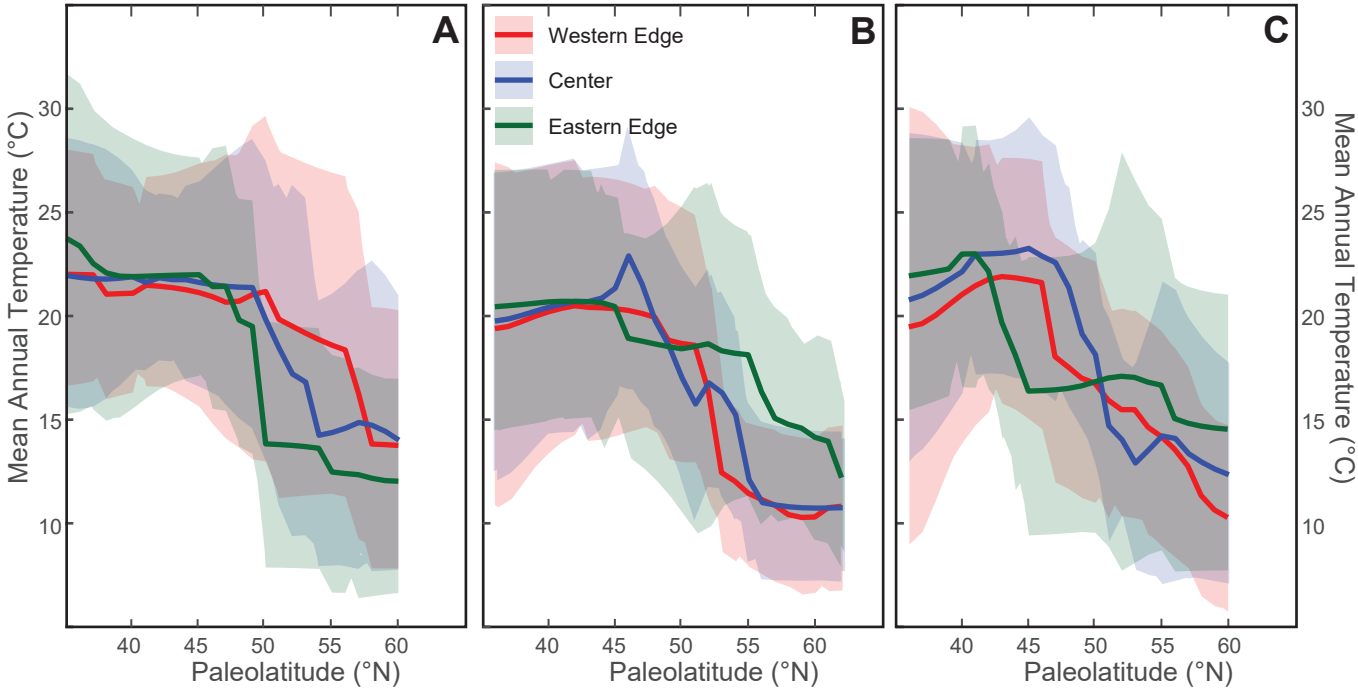
A
B
C
Western Edge
Center
Eastern Edge
Mean Annual Temperature (°C)
30
25
20
15
10
40
45
50
55
60
Paleolatitude (°N)

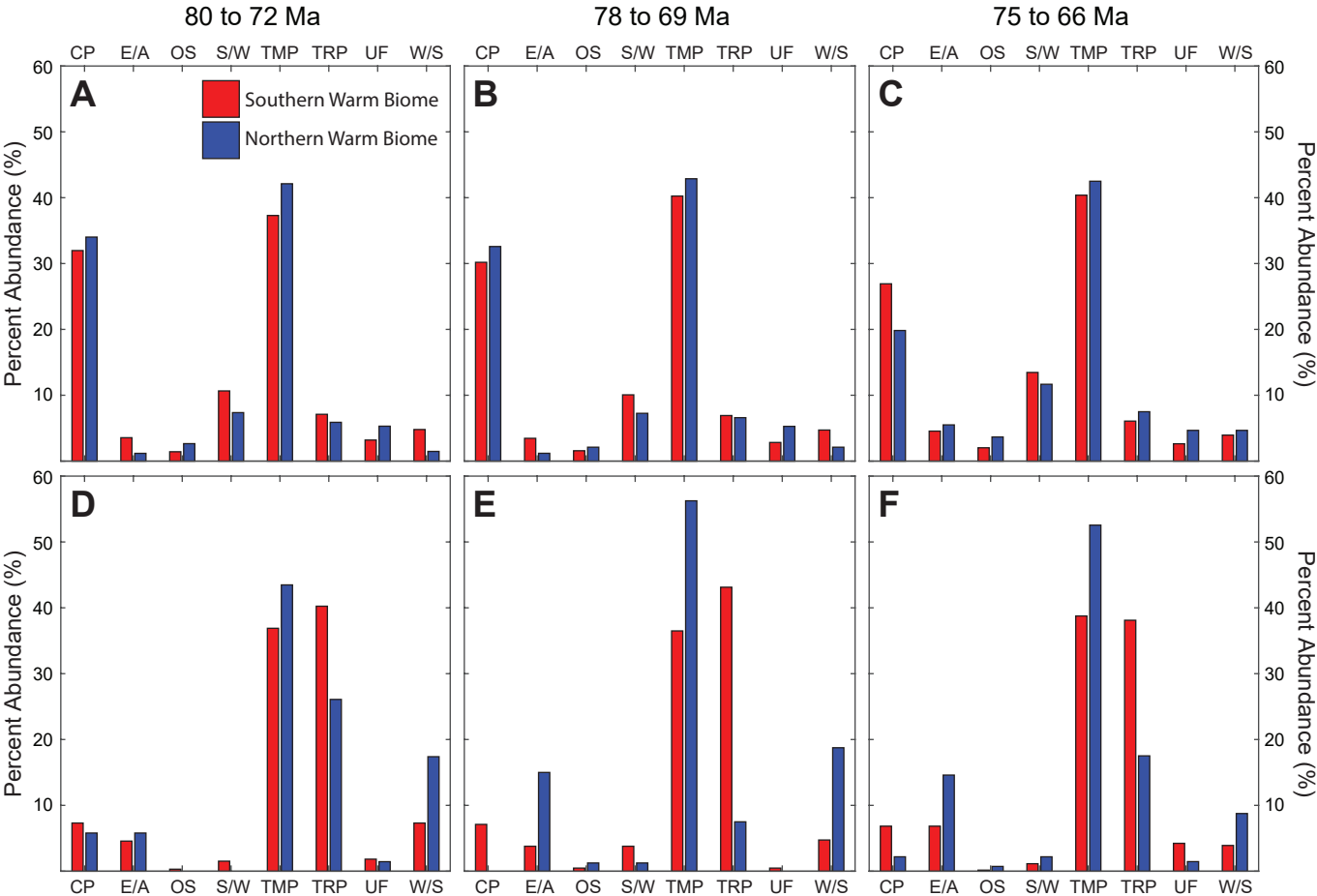
80 to 72 Ma
78 to 69 Ma
75 to 66 Ma
CP
E/A
OS
S/W
TMP
TRP
UF
W/S
A
B
C
D
E
F
Southern Warm Biome
Northern Warm Biome
Percent Abundance (%)
60
50
40
30
20
10

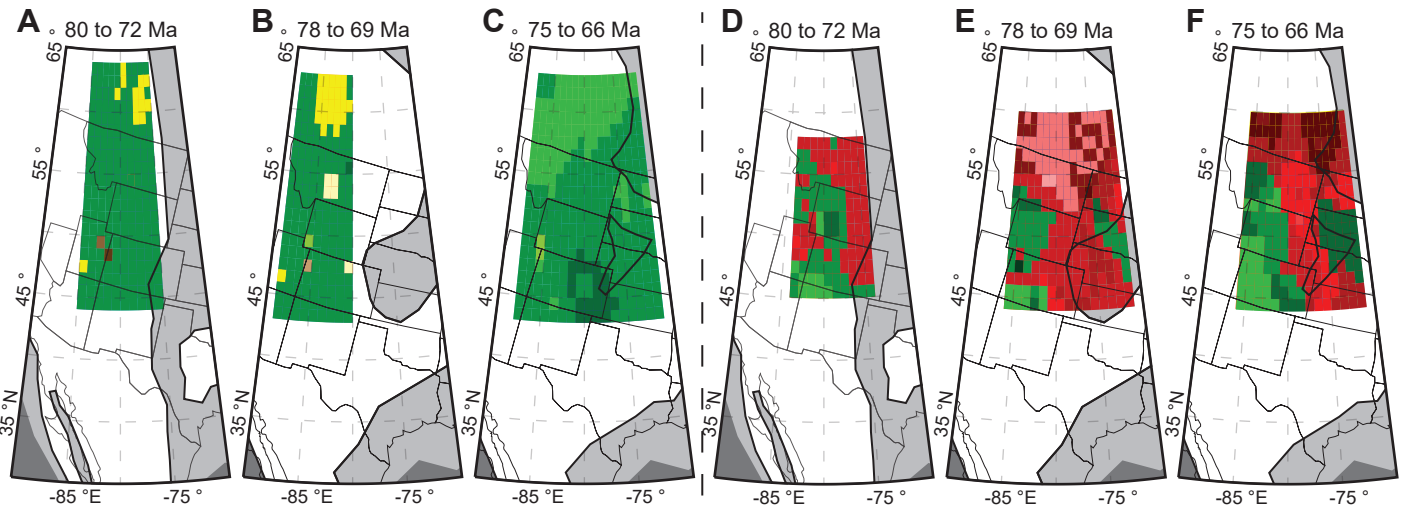

Mean (Min-Max) Ecotype abundance catogories:
I = 41% (33-50%); II = 30% (13-40%); III = 10% (7-16%); IV = 7% (2-12%)

- COASTAL PLAIN (I), TEMPERATE LOWLAND FOREST (II), SWAMPY OR LAGOONAL (III), OPEN SCRUBLAND (IV)
- COASTAL PLAIN (I), TEMPERATE LOWLAND FOREST (II), SWAMPY OR LAGOONAL (III), ESTUARINE OR AQUATIC (IV)
- COASTAL PLAIN (I), TEMPERATE LOWLAND FOREST (II), SWAMPY OR LAGOONAL (III), TROPICAL LOWLAND FOREST (IV)
- TEMPERATE LOWLAND FOREST (I), COASTAL PLAIN (II), TROPICAL LOWLAND FOREST (III), SWAMPY OR LAGOONAL (IV)
- TEMPERATE LOWLAND FOREST (I), COASTAL PLAIN (II), TROPICAL LOWLAND FOREST (III), SWAMPY OR LAGOONAL (IV)
- TEMPERATE LOWLAND FOREST (I), COASTAL PLAIN (II), WAMPY OR LAGOONAL (III), OPEN SCRUBLAND (IV)
- TEMPERATE LOWLAND FOREST (I), COASTAL PLAIN (II), WAMPY OR LAGOONAL (III), ESTUARINE OR AQUATIC (IV)
- TEMPERATE LOWLAND FOREST (I), COASTAL PLAIN (II), SWAMPY OR LAGOONAL (III), TROPICAL LOWLAND FOREST (IV)
- TEMPERATE LOWLAND FOREST (I), COASTAL PLAIN (II), SWAMPY OR LAGOONAL (III), UPLAND FOREST (IV)

Mean (Min-Max) Ecotype abundance catogories:
I = 48% (35-68%); II = 29% (11-47%)

- TROPICAL LOWLAND FOREST (I), WET OR SUCCESSIONAL (II), TEMPERATE LOWLAND FOREST (III)
- TROPICAL LOWLAND FOREST (I), TEMPERATE LOWLAND FOREST (II), ESTUARINE OR AQUATIC (III)
- TROPICAL LOWLAND FOREST (I), TEMPERATE LOWLAND FOREST (II), WET OR SUCESSIONAL (III)
- TROPICAL LOWLAND FOREST (I), TEMPERATE LOWLAND FOREST (II), COASTAL PLAIN (III)
- TEMPERATE LOWLAND FOREST (I), ESTUARINE OR AQUATIC (II), TROPICAL LOWLAND FOREST (III)
- TEMPERATE LOWLAND FOREST (I), ESTUARINE OR AQUATIC (II), WET OR SUCCESSIONAL (III)
- TEMPERATE LOWLAND FOREST (I), TROPICAL LOWLAND FOREST (II), ESTUARINE OR AQUATIC (III)
- TEMPERATE LOWLAND FOREST (I), TROPICAL LOWLAND FOREST (II), WET OR SUCCESSIONAL (III)
- TEMPERATE LOWLAND FOREST (I), TROPICAL LOWLAND FOREST (II), COASTAL PLAIN (III)
- TEMPERATE LOWLAND FOREST (I), TROPICAL LOWLAND FOREST (II), UPLAND FOREST (III)
- TEMPERATE LOWLAND FOREST (I), WET OR SUCCESSIONAL (II), ESTUARINE OR AQUATIC (III)
- TEMPERATE LOWLAND FOREST (I), WET OR SUCCESSIONAL (II), TROPICAL LOWLAND FOREST (III)